2003

Effect of Temperature on Cs+ Sorption and Desorption in Subsurface Sediments at the Hanford Site, U.S.A.

Chongxuan Liu
Pacific Northwest National Laboratory, chongxuan.liu@pnl.gov

John M. Zachara
Pacific Northwest National Laboratory, john.zachara@pnl.gov

Odeta Qafoku
Pacific Northwest National Laboratory

Steve Smith
Pacific Northwest National Laboratory

Liu, Chongxuan; Zachara, John M.; Qafoku, Odeta; and Smith, Steve, "Effect of Temperature on Cs+ Sorption and Desorption in Subsurface Sediments at the Hanford Site, U.S.A." (2003). *US Department of Energy Publications*. 222.
https://digitalcommons.unl.edu/usdoepub/222

Effect of Temperature on Cs$^+$ Sorption and Desorption in Subsurface Sediments at the Hanford Site, U.S.A.

CHONGXUAN LIU,* JOHN M. ZACHARA, ODETA QAFOKU, AND STEVE C. SMITH

Pacific Northwest National Laboratory, Richland, Washington 99352

The effects of temperature on Cs$^+$ sorption and desorption were investigated in subsurface sediments from the U.S. Department of Energy Hanford Site. The site has been contaminated at several locations by the accidental leakage of high-level nuclear waste (HLW) containing ^{137}Cs$^+$. The high temperature of the self-boiling, leaked HLW fluid and the continuous decay of various radionuclides carried by the waste supernatant have resulted in elevated vadose temperatures (currently up to 72 °C) below the Hanford S-SX tank farm that have dissipated slowly from the time of leakage (1970). The effect of temperature on Cs$^+$ sorption was evaluated through batch binary Cs$^+$−Na$^+$ exchange experiments on pristine sediments, while Cs$^+$ desorption was studied in column experiments using ^{137}Cs$^+$-contaminated sediments. Cs$^+$ adsorption generally decreased with increasing temperature, with a more apparent decrease at low aqueous Cs$^+$ concentration (10^{-10}–10^{-6} mol/L). Cs$^+$ desorption from the contaminated sediments increased with increasing temperature. The results indicated that the free energy of Na$^+$−Cs$^+$ exchange on the Hanford sediment had a significant enthalpy component that was estimated to be −17.87 (±2.01) and −4.82 (±0.44) kJ/mol (at 298 °C) for the high- and low-affinity exchange sites, respectively. Both Cs$^+$ adsorption and desorption at elevated temperature could be well simulated by a two-site ion exchange model, with the conditional exchange constants corrected by the exchange enthalpy effect. The effect of temperature on Cs$^+$ desorption kinetics was also evaluated using a stop-flow technique. The kinetics of desorption of the exchangeable pool (which was less than the total adsorbed concentration) were found to be rapid under the conditions studied.

Introduction

High-level nuclear waste (HLW) resulted from the reprocessing of irradiated uranium fuel for Pu extraction. Within the United States, millions of gallons of HLW remain in storage at U.S. Department of Energy facilities awaiting safe, long-term stabilization and disposal. The HLW are enriched in fission products including ^{137}Cs$^+$, ^{90}Sr^{2+}, and many other radionuclides. Some of the HLW were self-boiling for several years after reprocessing as a result of the decay of short half-life radionuclides. HLW has been accidentally released to the vadose zone at Hanford and other DOE sites as a result of tank overfilling, transfer line breakage, and tank failures. ^{137}Cs$^+$ is one of several contaminants of concern in these leak events. In this communication we evaluate the effects of temperature on Cs$^+$ adsorption and desorption from Hanford sediments. The research provides insights on the sorption chemistry of ^{137}Cs$^+$ in a HLW vadose zone plume at Hanford's S-SX tank farm that contains in excess of 1000 kCi of ^{137}Cs$^+$. Subsurface temperatures within this plume have remained in excess of 50 °C for over 30 years since the time of HLW leakage as a result of radioactive decay and the high thermal load of the self-boiling HLW. Figure 1 shows current vertical profiles of ^{137}Cs$^+$ and temperature proximate to tank SX-108.

Cesium strongly and preferentially adsorbs on 2:1 layer silicate minerals in soils and sediments (*1*−*3*). Cesium sorption on micaceous minerals such as illite (*4*, *5*) and sediments containing such minerals (*3*, *6*) has typically been treated as a cation exchange process involving two or more sites with distinctive exchange energies (high and low affinity). The high-affinity sites are believed to reside along the weathered edges or collapsed interlayer regions of micaceous minerals, while the low-affinity sites populate the basal and interlamellar regions of both nonexpansible and expansible phyllosilicates (e.g., vermiculites and smectites). The high affinity of Cs$^+$ for fixed charge sites on micaceous minerals results from the unique registry of the dehydrated Cs$^+$ ion with the ditrigonal siloxane cavity on high charge density phyllosilicates (*7*, *8*).

The effects of temperature on Cs$^+$ adsorption and desorption are not well established. Komarneni and Roy (*9*) found that hydrothermal treatment (200−400 °C at 300 bar) of shale or sediments containing vermiculite or illite decreased both Cs$^+$ adsorption and desorption. X-ray diffraction examination of the sediments indicated that the decrease in Cs$^+$ adsorption and desorption resulted from the collapse of edge-interlayer sites. This collapse reduced the number of sites available for adsorption and locked adsorbed Cs$^+$ within the structure, preventing desorption. Secondary Cs$^+$-containing minerals (i.e., CsAlSi$_2$O$_6$) resulting from hydrothermal treatment were also speculated to retard Cs$^+$ desorption in some cases (*10*, *11*).

We report here on the influence of temperature on Cs$^+$ adsorption to and desorption from Hanford sediment over the temperature range of 15−65 °C. Adsorption isotherms were measured in batch mode for Na$^+$−Cs$^+$ ion exchange on pristine Hanford sediments at variable temperature to characterize the temperature dependence of the adsorption process. Desorption experiments were performed using small columns packed with contaminated sediments containing 10^8 pCi/g ^{137}Cs$^+$ collected from beneath leaked Hanford tank SX-108. The sediment was contaminated by release of caustic, self-boiling HLW in 1970. The columns were leached with NaNO$_3$ (the primary electrolyte present in Hanford HLW) at various temperatures to evaluate the temperature dependence of desorption. A two-site ion exchange model that was developed and applied previously to sediments from this site (*3*, *6*, *12*) was used to interpret the results.

Materials and Methods

Sediment Collection and Analysis. Pristine core samples were collected from four monitoring wells surrounding the S-SX tank farm (*3*). The subsamples of the field-moist materials were air-dried to a constant weight and sieved to pass a 2-mm mesh. Gravels > 2 mm were removed from the

* Corresponding author phone: (509)376-0129; fax: (509)376-3650; e-mail: chongxuan.liu@pnl.gov. Corresponding address: Pacific Northwest National Laboratory, P.O. Box 999, MSIN K8-96, Richland, WA 99352.
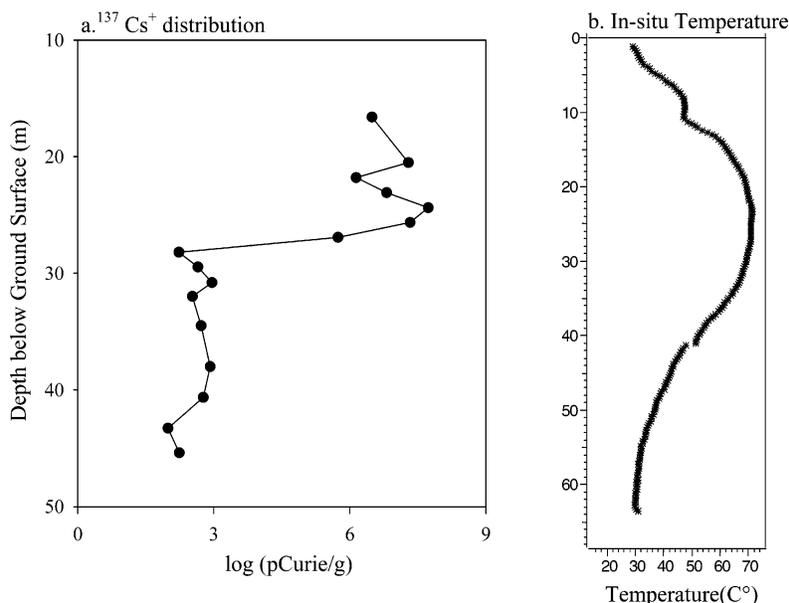
FIGURE 1. Vertical distribution of temperature and $^{137}Cs^+$ beneath tank SX-108 in the S-SX tank farm at the Hanford Site. The contaminated sample used in this study was from depth of 25.8 m below ground surface.

air-dried materials during the sieving process. The sieved materials were mixed thoroughly to obtain a homogeneous sample and were designated as the Above B composite. The cation exchange capacity (CEC) of the composite ranged from 4.26 to 8.25×10^{-5} equiv/g of dry soil as determined previously using different methods (3), and a value of 8.25×10^{-5} equiv/g was consistent with all previous experimental and modeling results of Cs^+ sorption and desorption at room temperature (3, 6).

The $^{137}Cs^+$-contaminated sediments were collected from Borehole SX-108 (a borehole near tank SX-108) in the Hanford S-SX tank farm at a sample location approximately 25.8 m below ground surface. The sample collection and analyses are described elsewhere (13). The subsamples were air-dried, sieved, and mixed following the same procedures used for the pristine sediments. Sediments both with and without Cs^+ contamination had the same mineral composition, except that certain mineral phases in the contaminated sediments were altered by reaction with alkaline HLW (12).

The mineralogy of the Hanford pristine sediment was described previously (3). Briefly, it consisted predominantly of quartz with lesser amounts of plagioclase and potassium feldspars, mica, chlorite, and smectite for particles larger than 2 μm. The clay fraction (<2 μm) consisted of smectite, chlorite, and mica. X-ray diffraction showed the micas to be muscovite, biotite, and vermiculitized biotite.

Cs^+ Sorption to NaOAc-Treated above B Sediment. The Above B sediment was treated with sodium acetate (NaOAc) at pH 4.5 to dissolve soluble salts and calcite, and to saturate the exchanger phase with Na^+. The detail experimental procedure for this treatment was described elsewhere (3). Cesium sorption on the treated Above B sediment was measured at three temperatures—30, 45, and 65 °C—in 0.1 mol/L $NaNO_3$ electrolyte. Previous exchange measurements (3) had been performed at 30 °C. The sorption experiments used a solid concentration of about 10 g/L and Cs^+ concentrations in the range of 10^{-1}–10^{-9} mol/L in $CsNO_3$ labeled with 7 to 20×10^3 dpm/mL $^{137}Cs^+$. The background Cs^+ in sediment suspensions of 0.1 mol/L $NaNO_3$ solution was below detection limit (1.1 μg/L) and was less than 1. $\times$ 10^{-9} mol/L estimated from the measurements of Cs^+ in 5 mol/L $NaNO_3$ solution (5.9 μg/L or 4.4×10^{-8} mol/L) and dilution trend from 5 mol/L to 1 mol/L $NaNO_3$ solutions. The suspensions were shaken in a 30-mL polycarbonate tube at 40 rpm for 16 h. After equilibration, the suspensions were centrifuged, and the supernatants were measured for $^{137}Cs^+$. The $^{137}Cs^+$ activity of the sample was counted for 30 min using a Wallac Model 1480 gamma counter with an 80-mm NaI crystal detector. The count window was set at 560−710 keV, yielding a count efficiency of 0.207. The sorbed Cs^+ was calculated from the difference between the initial and final aqueous concentrations of Cs^+.

Leaching of Cs^+ from the Contaminated Sediments. Approximately 2 g of air-dried sediments were packed into polypropylene columns 3.1 cm long $\times$ 0.78 cm in diameter. The columns were connected to a peristaltic pump on one side and a fraction collector on the other. Each column was inserted into a water jacket at a specific temperature. Immediately before the columns were connected to a leaching solution, approximately 10 mL of pure CO_2 gas was injected through the columns to displace air from the sediment pore space. A uniform movement of the leaching solution through the packed air-dried sediments was observed. Sediment leachates were collected every 6 min, and the mass of collected solutions was determined to validate the flow rate. After all the leachates were collected, the packed columns were flushed with deionized water and weighed; the sediment pore space was determined as a weight difference between wet and air-dried sediment. The ratio of dry solid weight to aqueous volume was 3.03×10^3 g/L in the packed column, a value corresponding to 0.47 porosity under an assumption of solid density of 2.65 kg/L. The concentration of $^{137}Cs^+$ in the leachates was measured as described above for Cs^+ sorption.

In one set of column desorption experiments, the sediments were leached continuously with 0.5 mol/L $NaNO_3$ for about 10 pore volumes at 15 °C and a flow rate of 0.1 mL/min. This flow rate yielded a residence time of 6 min. The temperature of the water jacket then was increased to 55 °C, and the sediments were leached continuously for another 10 pore volumes. At this time, a stop-flow method was applied for 2.5 h, followed by another 10 pore volumes of leaching before the temperature of the water jacket decreased to 35 °C. After leaching for about 10 pore volumes at 35 °C, the stop-flow method was applied again for 2.5 h, followed by continued leaching for about eight pore volumes before the temperature decreased to 15 °C. Similarly, the leaching at 15 °C was stopped for 2.5 h after 8 pore volumes and resumed
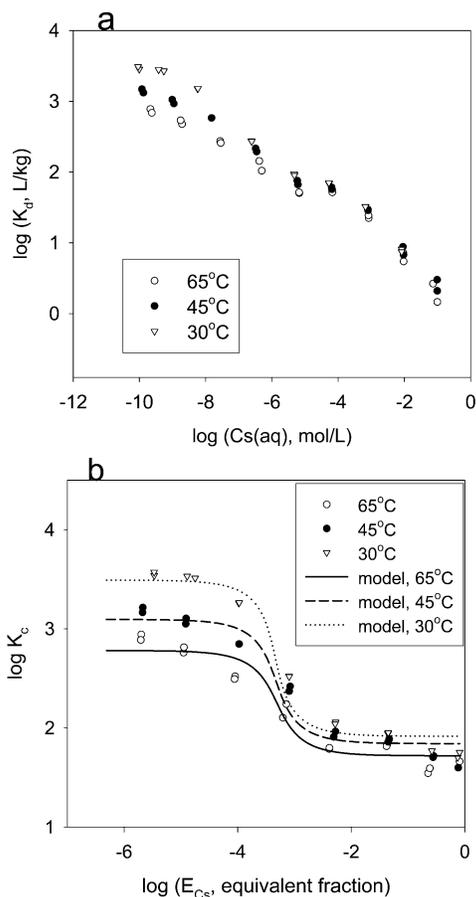
FIGURE 2. Cs$^+$ sorption in 0.1 mol/L NaNO$_3$ electrolyte on the NaOAc-treated pristine Hanford sediment: (a) Cs$^+$ distribution coefficient (K_d) as a function of temperature and equilibrium aqueous Cs$^+$ concentration; (b) experimental and modeling results of conditional exchange constant (K_c) as a function of temperature and equivalent Cs$^+$ fraction (E_{Cs}) on the solid phase.

for another eight pore volumes before termination. The other set of leaching experiments involved increasing the temperature from 15° to 35 °C and then to 55 °C in the water jacket. At the midpoint of the leaching process at each temperature, the flow was stopped for 2.5 h and then resumed as described above.

Results and Discussion

Effect of Temperature on Cs$^+$ Sorption. Cesium sorption, as measured by the concentration distribution ratio (K_d), increased with decreasing temperature at low-equilibrium aqueous Cs$^+$ concentration ($10^{-10}-10^{-5}$ mol/L) (Figure 2a). The measured K_d values nearly doubled at low concentration as temperature decreased from 45° to 30 °C and increased about five times from 65° to 30 °C. However, the K_d changes with temperature became smaller with increasing aqueous Cs$^+$ concentrations (>10^{-5} mol/L). These results indicated that temperature mainly affected Cs$^+$ sorption behavior in the high K_d region.

The conditional Cs$^+$ exchange coefficients (K_c) at different temperatures (Figure 2b) exhibited multisite exchange behavior, as observed previously at room temperature for pure illite (4) and sediments containing micaceous and smectite sorbents (3). The exchange reaction may be written as
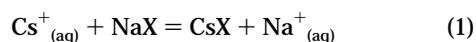
$$Cs^+_{(aq)} + NaX = CsX + Na^+_{(aq)} \quad (1)$$

TABLE 1. Parameters Estimated from Cs$^+$ Sorption Results at Variable Temperatures[a]

T (°C)	Log K_c (Cs$^+$ for Na$^+$) site I	site II	ΔH^o (kJ/mol) site I	site II	ΔS^o (J/mol K) site I	site II
30	6.827(0.066)	1.916(0.050)	−17.87	−4.82	−2.41	0.08
45	6.417(0.071)	1.842(0.055)	(2.01)	(0.44)	(6.49)	(1.41)
65	6.088(0.062)	1.719(0.047)				

[a] Numbers in parentheses are standard deviations.

where NaX and CsX are the exchanger phase species of Na$^+$ and Cs$^+$ and Cs$^+_{(aq)}$ and Na$^+_{(aq)}$ are aqueous species. The conditional exchange constant (K_c) was defined as

$$K_c = (N_{Cs}/N_{Na})([Na^+_{(aq)}]/[Cs^+_{(aq)}]) \quad (2)$$

where N_{Cs} and N_{Na} are the mole fractions on the exchanger phase, and [Cs$^+_{(aq)}$] and [Na$^+_{(aq)}$] are the aqueous concentrations for species Cs$^+$ and Na$^+$, respectively.

The K_c generally decreased with increasing temperature, with more apparent decreases in the high-affinity (high-K_c) region (Figure 2b). At each temperature, the K_c sharply decreased at an equivalent fraction [E_{Cs} = Cs$^+$(equiv/g)/CEC-(equiv/g)] of 5 × 10^{-4}. The inflection point of K_c was an indication of the saturation of the high-affinity exchange site. This inflection point has been used to estimate the capacity of that site (4). The observance of a common inflection point at each different temperature indicated that the equivalent fraction of the high-affinity site did not change with temperature. This result was in contrast with a previous observation (9) that the capacity of the high-affinity site sharply decreased with increasing temperature due to the collapse of the edge-interlayer region. The mild temperature change (30−65 °C) and low pressure (1 atm) of this study may explain such a difference.

Because of the step characteristic of the experimental K_c values at each temperature (Figure 2b), a two-site exchange model (3) was applied here to describe the Cs$^+$ sorption

$$K_c(E_{Cs}) = (b + \sqrt{b^2 + 4K_c^I K_c^{II} E_{Cs}(1 - E_{Cs})})/(2 - 2E_{Cs}) \quad (3)$$

where $b = (E^I - E_{Cs})K_c^I + (1 - E^I - E_{Cs})K_c^{II}$; K_c^I and K_c^{II} are the conditional exchange coefficients for site I and II, respectively; E^I is the fraction of the sediment CEC contributed by site I; and E_{Cs} is the equivalent fraction of total sorbed Cs$^+$ among CEC. The two-site exchange model could be well fitted to each Cs$^+$ sorption isotherm (Figure 2b) by adjusting the conditional exchange coefficients of the two sites. The high-affinity site fraction (E^I) was fixed at 4.5 × 10^{-5} for all temperatures, which was consistent with the observed inflection point of the K_c curves (Figure 2b). This same value of E^I has been used to successfully describe other experimental results with variable ionic strength and exchanging electrolytes for this sediment (6). With a fixed capacity of high-affinity sites (E^I), the change of the overall K_c at each temperature was attributed to the changes in the conditional exchange constants (eq 3) for both the high and low affinity Cs$^+$ exchange sites (Table 1).

The effects of temperature on the exchange constant (K_{ex}) may be described by the Gibbs−Helmholtz equation

$$\frac{\partial \ln K_{ex}}{\partial (1/T)} = -\frac{\Delta H}{R} \quad (4)$$

where ΔH is the enthalpy change for reaction 1 at temperature T and R is the gas constant. The K_{ex} is a function of the conditional exchange constant (eq 2) corrected by the activity
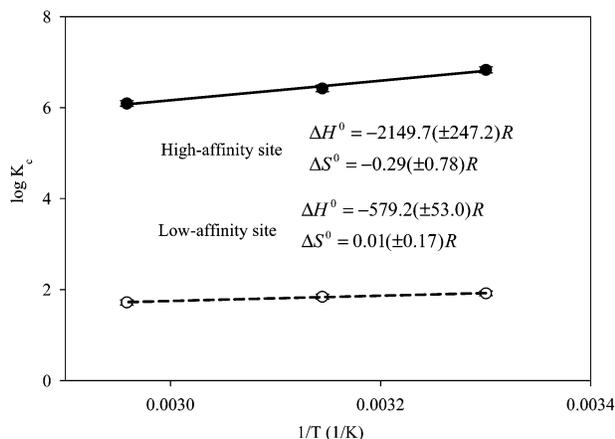
FIGURE 3. The relationship of the conditional exchange constants (K_c) of Cs$^+$ for Na$^+$ at the high and low affinity sites to inverse temperature.

coefficients of aqueous and exchanger phase species. The ion exchange of Cs$^+$ on Hanford sediments at room temperature was found to be nonideal and influenced by the water activity (6). However, the activity coefficient ratios for the aqueous and exchanger phase species canceled one another for homovalent exchange (e.g., Na$^+$−Cs$^+$). As a result, the K_c measured at different ionic strengths converged to a single line within the errors of experimental measurement in 0.1−5.0 mol/L NaNO$_3$ (3). Because of this observation and the unavailability of temperature-variable ion−ion interaction parameters for the aqueous species pairs such as Cs$^+$−Na$^+$ and Cs$^+$−NO$_3^-$, it was assumed in the following analysis that the activity coefficient ratios canceled one another at different temperatures so that K_{ex} in eq 4 could be replaced by K_c.

K_c (Table 1) showed a linear trend with $1/T$ for both the high and low affinity exchange sites (Figure 3). The linear relationship allowed us to approximate ΔH as a constant and to integrate eq 4 to obtain

$$\ln K_c = -\frac{\Delta H°}{RT} + \frac{\Delta S°}{R} \qquad (5)$$

where $\Delta H°$ and $\Delta S°$ are the standard enthalpy and entropy changes for reaction 1, respectively. After linearly fitting eq 5 to the results of K_c vs $1/T$ (Figure 3), we obtained $\Delta H° = -17.87$ (± 2.01) kJ/mol for the high-affinity site and -4.82 (± 0.44) kJ/mol for the low-affinity site (the values in bracket are standard deviations calculated from the variances of parameter estimates by linear regression). The estimated intercepts (or entropy changes $\Delta S°$, for the exchange reaction, eq 5) were small for both sites, and the estimated values were associated with large uncertainties (Table 1 and Figure 3).

Effect of Temperature on Cs$^+$ Desorption from the Contaminated Hanford Sediment. The concentration of Cs$^+$ in the column effluent from the contaminated sediment increased with increasing temperature (Figures 4 and 5), indicating that Cs$^+$ desorption increased with temperature. Each column displayed an initial high release of Cs$^+$ in the first two pore volumes (Figures 4 and 5), before the data converged on "step function" behavior. The initial pulse was caused by residual NaNO$_3$ (present as solid salt in the dried sediment) that dissolved in the 0.5 mol/L NaNO$_3$ leaching solution and increased its concentration. This increased Na concentration proportionally enhanced Cs$^+$ desorption. The residual NaNO$_3$ was completely dissolved in the first two pore volumes of leaching and after that point Na concentrations were constant and equal to those in the influent solutions (0.5 mol/L). The total Cs$^+$ concentrations in Figures
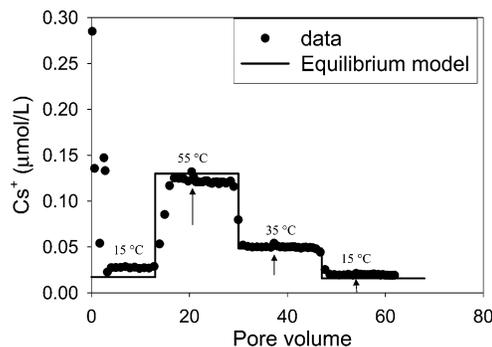

FIGURE 4. Effluent concentrations of Cs$^+$ from columns of contaminated Hanford sediment leached with 0.5 mol/L NaNO$_3$ at different temperatures as noted. Solid lines are model calculations. The stop-flow event (labeled by arrow) appears as a small increase in Cs$^+$ concentration midway through each temperature cycle.
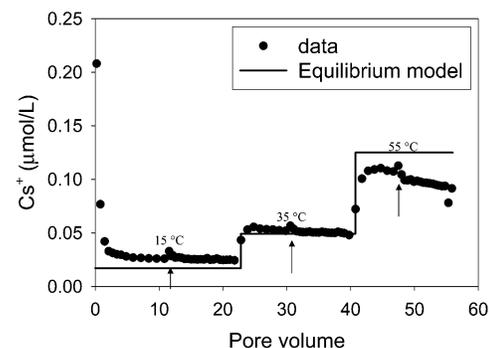

FIGURE 5. Effluent concentrations of Cs$^+$ from columns of contaminated Hanford sediment leached with 0.5 mol/L NaNO$_3$ at different temperatures as noted. Solid lines are model calculations. The stop-flow event (labeled by arrow) appears as a small increase in Cs$^+$ concentration midway through each temperature cycle.

4 and 5 were calculated from the measured concentrations of ^{137}Cs$^+$ using the following relationship to account for the contribution from other Cs$^+$ isotopes including 133 and 135 (12):

$$\text{Cs}^+ \text{ (mol/L)} = 4.748 \,^{137}\text{Cs}^+ \text{ (mol/L)} \qquad (6)$$

The molar concentration is related to the activity of ^{137}Cs$^+$ by

$$^{137}\text{Cs}^+ \text{ (mol/L)} = \\ ^{137}\text{Cs}^+ \text{ (dpm/L)}*365.25*24*60*t_{1/2}/(\ln 2*N_A) \qquad (7)$$

where $t_{1/2}$ is the half-life of ^{137}Cs$^+$ decay (30.07 years), and N_A is the Avogadro constant.

The Cs$^+$ breakthrough concentrations were generally constant at each temperature, except for the initial 1−2 pore volumes, indicating that the desorption rate was more rapid than the advective flux rate. The effluent concentration of Cs$^+$ increased slightly after 2.5 h of stop-flow at each temperature, but the concentrations rapidly returned to those measured prior to the stop-flow event. These results indicated that mass transfer effects on Cs$^+$ desorption were not significant at the advective flow rate used and within the experimental duration of 60 pore volumes.

There was a slight decrease in Cs$^+$ effluent concentration with time at 55 °C (Figure 4) and a more obvious decrease at 55 °C during the last stage of leaching (Figure 5). The cumulative mass outflow in the desorption experiments was calculated to be 7% (Figure 4) and 6% (Figure 5) of total Cs$^+$ associated with the sediment [2.372×10^{-8} mol/g (12)]. This quantity was less than the amount of exchangeable Cs$^+$

measured for these same sediments in batch experiments (*12*) (30−45% of total Cs$^+$). The exchangeable fraction included equilibrium and kinetically desorbable pools of Cs$^+$ within the sediment (*12*). These results indicated that large extent of Cs$^+$ desorption at 55 °C may have depleted the sorbed, equilibrium-exchangeable Cs$^+$ concentration to levels where the kinetically controlled, desorbable fraction of Cs$^+$ on the sediment became important. The rates of Cs$^+$ flux out of the column were 2.5, 5.0, and 11 × 10^{-12} mol/min at 15, 35, and 55 °C, respectively.

Increased Cs$^+$ desorption at higher temperature was consistent with the batch adsorption results observed using uncontaminated sediments (Figure 2). The decrease in the magnitude of the conditional exchange constants with increasing temperature allowed more mass action displacement of Cs$^+$ by Na$^+$ from the exchanger phase. This result, however, was again in contrast with the previous findings that Cs$^+$ desorption from sediments containing illite and vermiculite was decreased by high-temperature (>200 °C) treatment (*9, 11*). The decrease in desorption with increasing temperature was attributed to the edge-interlayer collapse (*9, 11*) and the formation of secondary Cs$^+$-containing alumino-silicate minerals at high temperature (*10, 11*). The results of this study, however, clearly indicated that edge-interlayer collapse and secondary mineral precipitation were not important relative to the enthalpy effect in our moderate temperature range (15−55 °C). The finding that temperature more strongly affects Cs$^+$ ion exchange on the high-affinity site (Figure 2) may explain why there were no apparent effects of temperature on Cs$^+$ sorption and desorption in montmorillonite (*14*) where only low affinity Cs$^+$ ion exchange sites are likely to exist.

The desorption results (Figures 4 and 5) were well simulated by the two-site equilibrium exchange model that was parametrized by ion exchange measurements on pristine sediment (Figure 2b). The relationship in eq 5 was used to estimate the conditional exchange constants as a function of temperature. It was also assumed that 64% of Cs$^+$ sorbed on the sediment was exchangeable. The CEC of 7.49 × 10^{-5} equiv/g of soil and the high-affinity site fraction of 5.7 × 10^{-4} determined previously (*12*) were used in the simulation. Soluble Na$^+$ and K$^+$ salts from HLW existed in the sediment (*12*), but these were not included in the simulation. As a result, the extent of Cs$^+$ desorption at the initiation of the experiment was under (not well)-simulated (Figures 4 and 5). The need to limit the desorbable fraction to 64% of the total sorbed Cs$^+$ concentration was an important part of the simulation. Comprehensive desorption studies of Cs$^+$ from these contaminated sediments have clearly shown that only a fraction of the absorbed pool is desorbable (*12*). Incomplete desorbability has been attributed to three major factors (*12*): collapse of the edge-interlayer region induced by the sorption of Cs$^+$ and/or K$^+$, armoring or blocking of Cs$^+$ sorption sites by the secondary alumino-silicates precipitated concurrently with or after Cs$^+$ adsorption, and slow diffusion of Cs$^+$ within interlayer regions.

Implication to Cs$^+$ Retardation and Migration in Field. This study has shown that temperature, through an exchange enthalpy effect on the high affinity site, can significantly influence the adsorption and desorption of Cs$^+$ within the in-ground Cs$^+$ pool (Figure 1). Increasing temperature makes the ion exchange reaction between sorbed Na$^+$ and aqueous Cs$^+$ less favorable. Accordingly, the retardation of Cs$^+$ by ion exchange is decreased, and its mobility is increased. K_d based calculations of the SX-108 ^{137}Cs$^+$ plume have always underestimated Cs$^+$ mobility, and various explanations have been advanced including colloid migration. The enhancement of radionuclide mobility by colloids including organic or inorganic particles in subsurface environments has been documented (*15−17*). The transport calculations have been
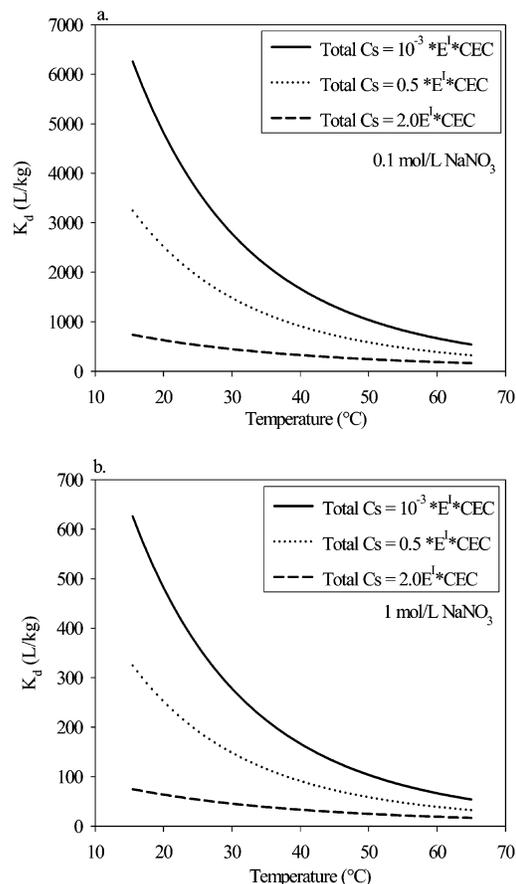

FIGURE 6. Simulation of the Cs$^+$ distribution coefficient (K_d) as a function of temperature and Cs$^+$ adsorption density. [A porosity of 0.47, high-affinity site fraction (E^I) of 5.7 × 10^{-4}, and sediment CEC of 7.49 mequiv/100 g corresponding to those in the leaching columns in Figures 4 and 5 were used in the simulation.] (a) and (b) show K_d in 0.1 and 1 mol/L NaNO$_3$ electrolytes, respectively.

based on sorption/ion exchange measurements (e.g., K_d) performed at room temperature. New results presented herein indicate that Cs$^+$ retardation at the 73 °C temperature observed in the core of the HLW plume would be well below that observed at 25 °C, all other conditions being equal. An interesting consequence of the temperature effects noted here is that the in-ground retardation of ^{137}Cs$^+$ will increase in the future as the temperature of the vadose zone decreases through heat dissipation. This phenomenon will further contribute to the in-situ immobilization of ^{137}Cs$^+$.

The temperature effect was caused by the large enthalpy change of the exchange reaction at the high-affinity site where Cs$^+$ was sorbed preferentially. Because of the low concentration of the high-affinity site in Hanford sediment (e.g., ∼4 × 10^{-8} equiv/g) the effect of temperature on the Cs$^+$ distribution coefficient (K_d) is dependent on adsorption density, as shown by numerical simulation (Figure 6). The effect of the ionic strength on the selectivity coefficients was neglected in the simulation. The K_d decreases with increasing temperature when the adsorption density is below the capacity of the high-affinity site. The decrease is markedly less when the adsorption density of Cs$^+$ is at or above the high affinity site capacity, because Cs$^+$ adsorption on the low affinity sites shows little temperature dependence. The Hanford Cs$^+$ plume (e.g., Figure 1) is clearly susceptible to temperature effects because the combined adsorption density of all Cs$^+$ isotopes (8.8 × 10^{-10}−2.4 × 10^{-8} mol/g) is below the total concentration of high affinity sites (∼4 × 10^{-8} mol/g) (Figure 6).

This study also showed that Cs^+ desorption from sediment that had been contaminated for over 30 yr could be well modeled by an equilibrium two-site exchange model corrected by the enthalpy effect up to 60 pore volumes of fluid passage. This volume of leaching solution is orders of magnitude above that expected for the Hanford vadose zone where natural recharge averages approximately 11 mm/yr because of a semi-arid climate. The column desorption study was performed at a porewater velocity (0.2 cm/min), that was much faster than typically observed in a silty sand aquifer (<0.1 cm/min) (18). Therefore, over normal ranges in porewater velocity found in the vadose zone and groundwater, Cs^+ sorption and desorption in contaminated Hanford sediment can be accurately described as an equilibrium mass exchange reaction between aqueous and solid phases. The most critical unknown variable is the exchangeable fraction of Cs^+, and insufficient measurements have been performed to predict this variable. A kinetic release model, such as that developed in ref 12, would be needed to predict Cs^+ migration in this particular plume (e.g., SX-108 at Hanford) if large volumes of water were to pass through the sediment (e.g., >60 pore volumes) or if leaching were to occur at rapid rate.

Acknowledgments

Literature Cited

(1) Sawhney, B. L. *Clays Clay Miner.* **1972**, *20*, 93−100.
(2) Francis, C. W.; Brinkley, F. S. *Nature* **1976**, *260*, 511−513.
(3) Zachara, J. M.; Smith, S. C.; Liu, C.; McKinley, J. P.; Serne, R. J.; Gassman, P. L. *Geochim. Cosmochim. Acta* **2002**, *66*, 193−211.
(4) Brouwer, E.; Baeyens, B.; Maes, A.; Cremers, A. *J. Phys. Chem.* **1983**, *87*, 1213−1219.
(5) Poinssot, C.; Baeyens, B.; Bradbury, M. H. *Geochim. Cosmochim. Acta* **1999**, *63*, 3217−3227.
(6) Liu, C.; Zachara, J. M.; Smith, S. C. *J. Contam. Hydrol.* **2003**, submitted.
(7) Eberl, D. D. *Clays Clay Miner.* **1980**, *28*, 161−172.
(8) Onodera, Y.; Iwasaki, T.; Ebina, T.; Hayashi, H.; Torii, K.; Chatterjee, A.; Mimura, H. *J. Contam. Hydrol.* **1998**, *35*, 131−140.
(9) Komarneni, S.; Roy, D. M. *Clays Clay Miner.* **1980**, *28*, 142−148.
(10) Brown, D. L.; Haines, R. I.; Owen, D. G.; Stanchell, F. W.; Watson, D. G. In *Geochemical Behavior of Disposed Radioactive Waste*; Barney, G. S., Navratil, J. D., Schulz, W. W., Eds.; American Chemical Society: Washington, DC, 1984; pp 217−227.
(11) Komarneni, S.; White, W. B. *Clays Clay Miner.* **1981**, *29*, 299−308.
(12) Liu, C.; Zachara, J. M.; Smith, S. C.; McKinley, J. P.; Ainsworth, C. C. *Geochim. Cosmochim. Acta* **2003**, in press.
(13) Serne, R. J.; Schaef, H. T.; Last, G. V.; Lanigan, D. C.; Lindenmeier, C. W.; Clayton, R. E.; LeGore, V. L.; O'Hara, M. J.; Brown, C. F.; Orr, R. D.; Kutnyakov, I. V.; Wilson, T. C.; Burke, D. B.; Williams, B. A.; Bjornstad, B. N. *Geologic and Geochemical Data Collected from Vadose Zone Sediments from the Slant Borehole under SX-108 in the S/SX Waste Management Area and Preliminary Interpretations*; Pacific Northwest National Lab: 2001.
(14) Andersson, K.; Torstenfelt, B.; Allard, B. *Sorption of radionuclides in geologic systems*; 1983.
(15) Lieser, K. H.; Gleitsman, B.; Peschke, S.; Steinkopf, T. *Radiochim. Acta* **1986**, *40*, 39−47.
(16) Marley, N. A.; Gaffney, J. S.; Orlandini, K. A.; Cunningham, M. M. *Environ. Sci. Technol.* **1993**, *27*, 2456−2461.
(17) McCarty, J. K.; Czerwinski, K. R.; Sanford, W. E.; Jardine, P. M.; Marsh, J. D. *J. Contam. Hydrol.* **1998**, *30*, 49−77.
(18) Freeze, R. A.; Cherry, J. A. *Groundwater*; Prentice-Hall: Englewood Cliffs, NJ, 1979.